FUSION OF ASCENDING AND DESCENDING POLARIMETRIC SAR DATA FOR COLOUR ORTHOPHOTO GENERATION

J. Zhang [a, *], J. Wei [a,b], G. Huang [a], Y. Zhang [a]

[a] Chinese Academy of Surveying and Mapping, Beijing, 100830, P.R.China - zhangjx@casm.ac.cn
[b] Liaoning Technical University, Fuxin, Liaoning Province, 123000, P.R.China

KEY WORDS: SAR, Orthorectification, Polarization, Fusion, Radiometric

ABSTRACT:

Synthetic Aperture Radar (SAR) is an effective earth observation sensor for the regions where frequent cloud and fog cover makes optical image acquisition extremely difficult. The State Bureau of Surveying and Mapping of China is conducting the western China mapping project, which aims to generate 1:50,000 scale topography and other thematic maps for the wild western china region covering around 2 million square kilometers and having not been mapped at this or finer scale before. A part of the western china region characterized by frequent cloud, fog and high mountains will be mapped by SAR. But, due to the inherent side-looking, SAR images suffer strong geometric distortions, such as layover, shadow and foreshortening, especially over mountainous regions. These geometric distortions greatly limited the interpretation of SAR images. To cope with this difficulty, a methodology of generating color SAR orthophotos over mountainous area has been proposed. The methodology consists of several important processes. A fully polarized SAR image is processed to form a color image, which generally has better interpretability than a gray-scale image from single polarized data. The color image is then ortho-rectified with high precision Digital Elevation Model (DEM). At the same time, the radiometric distortion induced by topography, e.g. the variation of effective illumination area within a pixel cell is corrected. Finally, two SAR images with opposite viewing angle, such as the ascending and descending acquisitions, are processed. A mask marking the layover and shadow area is generated based on the DEM. The ascending and descending SAR images are fused by replacing the pixels within the mask with those from the opposite viewing image. Through these processing, a colorful SAR orthophoto is generated, which can be used as a base map for image interpretation. The validity of the proposed methodology has been demonstrated with an experiment using RADARSAT-2 quad-polarization products in the Hengduan mountain area of Western China. A software module has been developed based on the methodology, and has been successfully applied to the Western China Mapping Project.

1. INTRODUCTION

SAR provides an efficient way of earth observation for areas covered by rain, haze/fog and cloud frequently through the year. However, SAR images have severe geometric distortions, such as layover and shadow, which are the consequences of side-looking viewing geometry and underlying topography relief. Precise geometric correction is thus absolutely necessary when spatial information of terrain feature is needed or an integrated analysis of multi-temporal and multi-source information is to be performed (Chen 2004). Since the prevalence of layover and shadow in mountainous areas, scattering signals from these distortion regions hardly contain information about terrain cover types. The State Bureau of Surveying and Mapping (SBSM) of China is conducting the Western China Mapping Project, which aims to generate 1:50,000 scale topography and other thematic maps for the wild western china region covering around 2 million square kilometers and having not been mapped at this or finer scale before. A part of the western china region characterized by frequent cloud, fog and high mountains, for example the Hengduan mountain area, will be mapped by SAR. Obviously, using a single SAR acquisition can not meet the needs of interpreting land cover and other thematic information in these regions. In this paper, a methodology is proposed to generating color SAR orthophotos by fusion two SAR acquisitions with opposite viewing geometry, e.g. the ascending and descending configuration.

* Corresponding author

2. METHODOLOGY OVERVIEW

The proposed methodology consists of several main processing steps: color composition from polarized SAR, ortho-rectification, terrain-induced radiometric correction, fusion of ascending and descending data. The overall flowchart of the methodology is shown in Fig.1. These processing steps are introduced as follows (Figure 1).

2.1 Color Composition of Polarized SAR

A polarimetric SAR measures the microwave reflectivity of a target using quad-polarizations HH, HV, VH, and VV to form a scattering matrix (Lee 1999). Based on the scattering matrix, many methods can be used to form a false color composite. In this work, the Pauli polarimetric decomposition method is used to generate the Red/Green/Blue channels as shown in Equation 1.

$$\begin{aligned} |a|^2 &\rightarrow \text{Blue} \\ |b|^2 &\rightarrow \text{Red} \\ |c|^2 &\rightarrow \text{Green} \end{aligned} \qquad (1)$$

Where $[a \quad b \quad c] = \frac{1}{\sqrt{2}}(S_{HH} + S_{VV} \quad S_{HH} - S_{VV} \quad 2S_{HV})$, and S_{HH}, S_{HV}, S_{VH}, S_{VV} are the elements of scattering matrix.

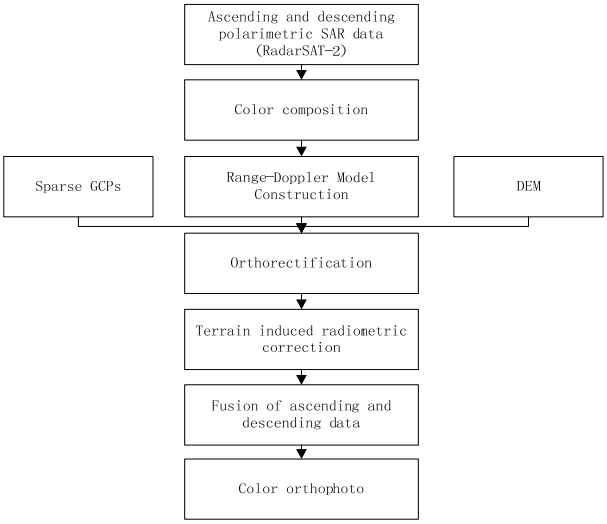

Figure 1. Flowchart of fusion of ascending and descending polarimetric SAR data for color orthophoto generation

2.2 SAR Imagery Ortho-Rectification with Sparse Ground Control Points (GCPs)

The Range-Doppler(R-D) equations (See equation 2) are the physical geometric model for SAR images. For spaceborne SAR, the R-D model can be calculated from the parameters provided in the header file of a SAR image. Based on the model, for every ground resolution cell represented by the 3D geodetic coordinate (X_m, Y_m, H_m), the projected image coordinate (i_c, j_c) can be calculated.

$$\begin{cases} R = |R_s - R_t| \\ f_d = -\dfrac{2}{\lambda}\dfrac{(R_s - R_t)V_s}{|R_s - R_t|} \end{cases} \quad (2)$$

In Equation 2, R_s and V_s are the position vector of the sensor(X_s, Y_s, Z_s)and velocity vector (X_v, Y_v, Z_v) respectively, R_t is the position vector of the ground target (X_t, Y_t, Z_t), R is the distance between the target and the sensor, f_d is the Doppler frequency of the center of the electromagnetic beam and λ is the wavelength of the electromagnetic wave.

But, due to the limited accuracy of the parameters provided in the header file, the calculated image coordinate (i_c, j_c) may offset from the real image coordinate (i_r, j_r), which corresponds to the ground target at (X_m, Y_m, H_m). The relationship between the calculated image coordinate and the real image coordinate can be modeled with a second-order polynomial expressed by equation 3. By means of at least 4 GCPs, these parameters (c_i , d_i) can be estimated using a least-square method. After knowing these parameters, the SAR image can be ortho-rectified to a known DEM (Y. Zhang 2002). Please note, here sparse GCPs are considered, because it is very difficult to obtain many GCPs given the remoteness and inaccessibility of the Western China region.

$$\begin{cases} i_r = c_0 + c_1 \times i_c + c_2 \times i_c^2 \\ j_r = d_0 + d_1 \times j_c + d_2 \times j_c^2 \end{cases} \quad (3)$$

2.3 Terrain Induced Radiometric Correction

It is assumed that the topography is flat in conventional SAR image radiometric calibration. In mountainous areas, the backscattering is distorted by topography relief (Y. Zhang 2003). As for space-borne SAR imagery, the radiometric distortion caused by topography is mainly the variation of effective scattering area. Theoretically speaking, the radiometric distortion caused by the scattering area reach a maximum when the local incident angle is zero. The smaller the incident angle, the bigger the error caused by the topography (Chen 2002). Considering this, we adopt the method proposed by Y. Zhang (2003) to correct the radiometric distortions caused by topography. This method involves calculate a scattering area normalization factor based on DEM and SAR imaging geometry.

The effective scattering area, namely A, is the area a SAR ground resolution cell in actual terrain projected to the normal plane of radar light. It can be calculated in Equation 4 (Adrian 1998).

$$A = \frac{\delta_r}{\sin(\eta_r)}\frac{\delta_a}{\cos(\theta_a)} \quad (4)$$

Where, δ_r is the slant resolution in range direction; δ_a is the azimuth resolution; η_r is the local incident angle in range direction; θ_a is the slope angle in azimuth direction.

As shown in Figure 2, η_r can be calculated according to Equation 5:

$$\eta_r = \gamma - \theta_r \quad (5)$$

where γ is the viewing angle of SAR, and θ_r is the slope angle in range direction.

Since the backscattering coefficient has a square relationship with the amplitude of SAR image, the amplitude value can be multiplied by a scattering area normalization factor σ expressed in equation 6 (Zhang Y 2002) to eliminate the radiometric distortion caused by the variation of effective scattering area of SAR ground cell.

$$\sigma = \sqrt{\sin(\gamma - \theta_r)\cos\theta_a} \quad (6)$$

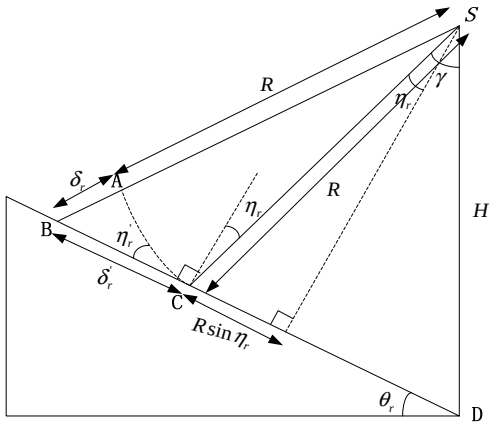

Figure 2. Local incident angle in range direction

2.4 Fusion of Ascending and Descending Images

Based on the terrain slope and aspect angles, a mask image can be generated which marks the areas affected by shadow

and layover. Since the radar illumination rays of ascending and descending images are opposite to each other, the masks will be complement to each other. Therefore the ascending and descending images can be fused by setting a decision rule to exclude pixels in layover/shadow region. The result image will be full of information and can be used for further interpretation. The details of this processing are introduced in next section.

3. FUSION OF ASCENDING AND DESCENDING SAR IMAGES

3.1 Basic Principle

Because of rough topography, there are severe layover and shadows in ortho-rectified SAR images. Figure 3 shows this phenomenon in ascending and descending SAR images in the Hengduan Mountain areas. Layover and shadow region has very limited useful information, which not only reduces the visual effect, but also results in the difficulty of image interpretation. However, since the lines of sight (LOS) of ascending and descending images are symmetry, the slopes facing the LOS of an ascending image are in the back slopes of corresponding descending image, vice versa. For example, figure 3(a) is a right side-looking SAR image in ascending direction and figure 3(b) is a descending one. The layover area surrounded by the red line in the facing slope in figure 3(a) corresponds to the red area in the back slope in figure 3(b). Therefore, the layover area in figure 3(a) can be substituted by the red area in figure 3(b), and similarly the layover area in figure 3(b) can also be replaced by the corresponding area in the back slope in figure 3(a). By compensating the layover/shadow region of ascending/descending data with the information from counterpart descending/ascending data, a SAR orthophoto with full information can be generated.

Based on the above principle, in this paper a new data fusion method using ascending and descending side-looking SAR images is proposed, including two parts: 1) detection of layover and shadow from SAR images; and 2) data fusion for ascending and descending SAR images.

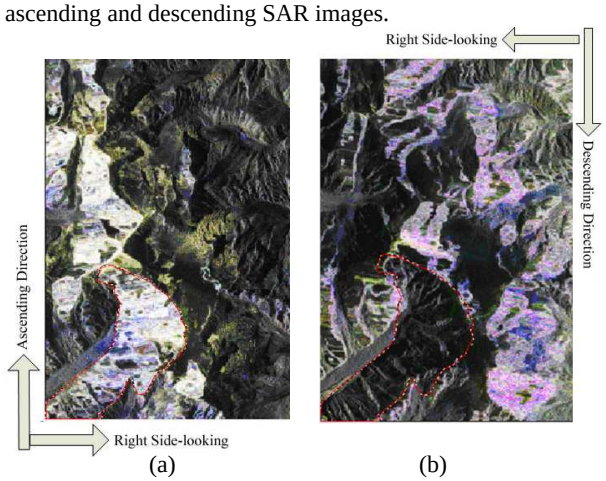

(a) (b)

Figure 3. (a) Ascending SAR images (b) Descending SAR images

3.2 Detection of layover and shadow

Layover and shadow areas in SAR image need to be detected before fusing ascending and descending data. Based on the SAR geometric model and DEM, a method is developed to detect layover and shadow areas from SAR images. The method includes the following steps:

1) The SAR image with larger incidence angle of the image center is selected as master image, and the other as the slave.

2) Using DEM, the aspect angle in azimuth direction of a pixel in the ortho-rectified master image is calculated, by means of which to determine whether this pixel is located in the facing slope or the back slope.

3) Based on the SAR geometric model, the original row and column coordinates of each pixel in the ortho-rectified master image are calculated. Accordingly, their satellite state vectors can also be obtained by utilizing orbit model.

4) Calculating look angle γ and slope angle θ_r in range direction. If the pixel is located in back slope and satisfies the condition $\theta_r > \gamma$, then it is within shadow area and marked as Flag =1. If the pixel is in the facing slope and meets the condition $\gamma + \theta_r \geq 90^o$, then it is determined to be within the layover area and marked as Flag=0.

5) Generating mask images. The mask images for layover and shadow are generated by conducting the calculation of step 2) ~ 4) for each pixel.

6) Editing the mask images. By means of morphological operations such as erosion, dilation and average filtering, the mask images are edited to eliminate the “islands” and “zigzags”, errors.

The method of detecting for layover and shadow areas mainly involves the following aspects: the judge rules for the facing and back slope, the calculation of radar look angle γ, slope angle in azimuth θ_a and slope angle θ_r in range.

1) Judge rules for the facing and back slope

(1) Heading angle calculation of SAR orbit

Heading angle Ω_s can be calculated with the first and last state vectors which are obtained from the leader file of master image.

(2) Base on DEM, aspect angle β_n of each pixel at ground resolution is calculated.

(3) Calculating the aspect angle in azimuth β_s for each pixel.

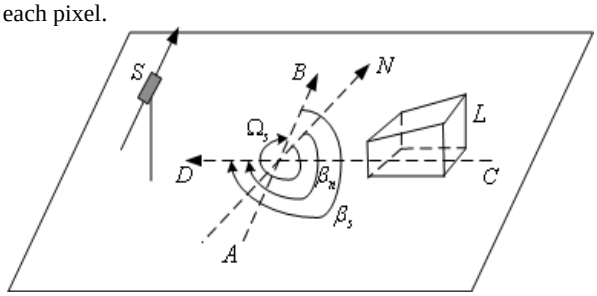

Figure 4. Aspect angle in azimuth direction

The aspect angle in azimuth β_s refers to the angle from flight direction of SAR sensor S to the aspect of ground resolution

pixel L . As shown in Figure 4, $\overrightarrow{AB}$ is parallel to the ascending orbit direction of SAR sensor S , N for the geographic north direction, β_n for the aspect angle of ground resolution pixel L , Ω_s for the heading angle of sensor S . Thus, the aspect angle in azimuth β_s can be expressed as:

a) If aspect angle β_n is greater than heading angle of sensor S , then

$$\beta_s = \beta_n - \Omega_s \quad (7)$$

b) If aspect angle β_n is less than or equal to heading angle of sensor S , then

$$\beta_s = 360 - \Omega_s + \beta_n \quad (8)$$

(4) To determine whether β_s is greater than 180° for each pixel, if YES, the pixel is judged to be in the facing slope, otherwise the back slope.

2) Calculation of radar look angle γ

Based on SAR imaging geometry, radar look angle γ can be expressed as (Jia 2005)

$$\gamma = 90^o - \arccos[\frac{|R_s|^2 + R^2 - |R_T|^2}{2\times|R_s|\times R}] \quad (9)$$

3) Calculation of slope angle θ_a in azimuth and slope angle θ_r in range

θ_a and θ_r are calculated with slope angle, aspect, and heading angle of SAR sensor, which are extracted from DEM.

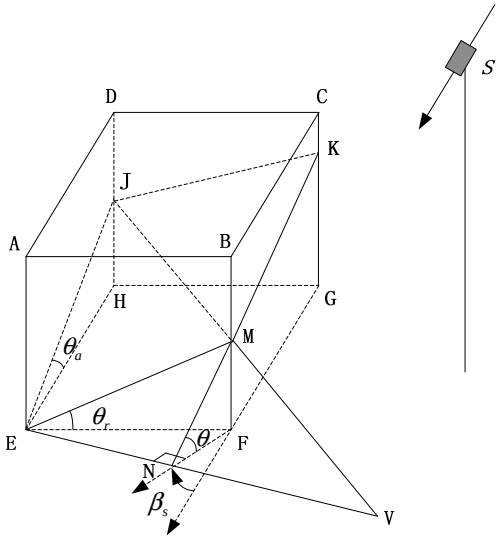

Figure 5. Slope angle θ_a in azimuth and slope angle θ_r in range

As shown in Figure 5, S is the SAR sensor. In the cuboid $ABCD-EFGH$, $\overrightarrow{GF}$ is parallel to the descending azimuth direction, and $\overrightarrow{FN}$ is the aspect of the ground scattering unit $EMKJ$, β_s is the azimuth angle of $\overrightarrow{FN}$ referring to the sensor flight direction $\overrightarrow{GF}$, θ_a and θ_r are the slope angles in azimuth and range of the ground scattering unit $EMKJ$, respectively. According to geometric relationship (Adrian 1998), we have

$$\tan(\theta_r) = \frac{MF}{EF} = \frac{MN\cdot\sin\theta\cdot\sin\beta_s}{MN\cdot\cos\theta} = \frac{\sin\theta\cdot\sin\beta_s}{\cos\theta} \quad (10)$$

Thus,

$$\theta_r = \arctan[\frac{\sin\theta\cdot\sin\beta_s}{\cos\theta}] \quad (11)$$

By the same way,

$$\theta_a = \arctan[\frac{\sin\theta\cdot\cos\beta_s}{\cos\theta}] \quad (12)$$

3.3 Data Fusion of Ascending and Descending SAR Images

The decision-making rule is shown is figure 6, using mask images for layover and shadow, by which the gray value of the pixel in layover and shadow areas can be replaced with corresponding pixel for multi-side-looking SAR data fusion.

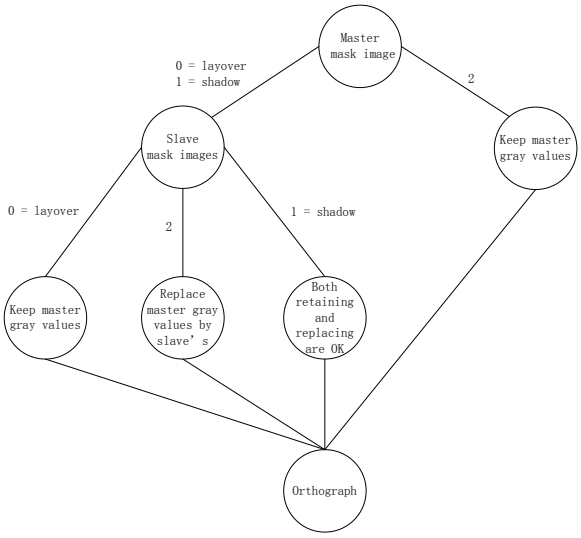

Figure 6. Fusion of ascending and descending SAR images

4. EXPERIMENT ANALYSIS AND APPLICATION

4.1 Test Area and Data

Based on the methodology and algorithms discussed above, a specific module has been developed. An experiment has been conducted using two RadarSat-2 (ascending track and descending track respectively) fully polarized images with 8m resolution in Hengduan Mountain area (see Fig. 7) to test the validity of the proposed methodology and the developed software.

Hengduan mountain area as a whole shows an east-west to north-south direction. It is characterized with high mountains, deep valleys, and complex landform types. The test area has a elevation varying from 1658 meters to 6719 meters above see level and the average 3642 meters. This topography has led to the severe foreshortening, layover and shadows in both the ascending and descending SAR images. The test area has very long time cloudy/foggy weather during a year, and

some meteorological disasters (thunder, snow and hailstone) occurs very often.

The complex topography and harsh natural conditions make traditional field work extremely hard. It is impossible to survey many GCPs in the field .Therefore, some points with clear visual feature at the Radarsat-2 images are seleted from SPOT-5 HRS panchromatic image (5 meters resolution) to be used as GCPs. Totally, 19 points are located with their planimetric coordinates measured from ortho-rectified SPOT 5 image and height from existing 1:100,000 DEM. Out of them, 5 points are used as GCPs to rectify the Radarsat-2 images with the method presented at section 2.2, and the rest 14 points are used as check points. The planimetric positioning accuracy of the rectification in the X direction is about 8m, in the Y direction about 7.5m, and the RMS is around 11m, which fully meets the standards of 1:50000 scale topography map regulated by SBSM.

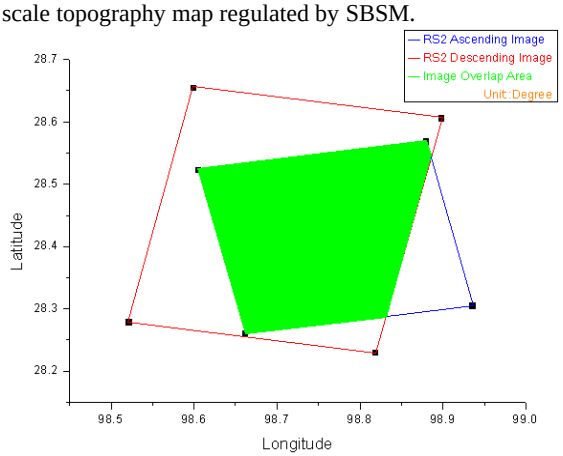

Figure 7. Spatial coverage of the ascending and descending RadarSat-2 images

4.2 Experiment Results and Analysis

4.2.1 Shadow and layover area detection According to the method of shadow and layover detection introduced in section 3.2, the ascending RadarSAT-2 image is chosen as the master image, and the descending one as the slave image. With the existing 1:100,000 DEM of the measured area, the shadow and layover areas of the SAR images are extracted as the mask map (as shown in Figure 8).

Figure 8. Mask map

Due to the limited accuracy of sensor orbit and DEM, for example the DEM we have used is at 1:100,000 scale, which generally has a grid spacing of 50 meters, the extracted mask map will present some errors, such as holes and zigzag. In order to reduce the impact of these errors on the afterward fusion process, the morphological erosion and dilation operations is used to filter the mask image. The effect of the morphological filtering is shown in Fig. 9.

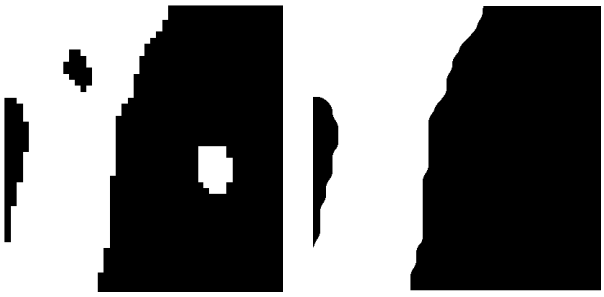

(a) (b)

Figure 9. (a)Original mask with hole and zigzag (b)After morphological filtering

4.2.2 Fusion of ascending and descending SAR images With the mask map of shadow and layover, the ascending image as the master image, the descending one as the subordinate image, the fusion experiment is carried out under integrated decision-making rules. The result is shown in Figure 10.

Figure 10(c) is the resulted SAR color orthophoto after image fusion. Figure 10(a) and Figure 10(b) are the ascending and descending rectified RadarSAT-2 image respectively. These figures show that after image fusion, the shadow and layover areas have been greatly mitigated and eventually a better color SAR orthophoto has been obtained. Moreover, this method is also applicable to the case of fusing moscaiced or subset images from different tracks, to cover a larger or only a portion of SAR frame.

4.3 Application

Based on the proposed methodology of color SAR orthophoto generation, the SAR color orthophotos covering 700,000 square kilometers in the Hengduan Mountain areas have been produced. These orthophotos have been used as the base map of field work to investigate the land cover and thematic information in this mountainous region.

5. DISCUSSION AND CONCLUSION

In Fig10(c), there are still some residual layovers and shadows, which are mainly caused by the following reasons:

1) The incidence angles of the ascending and descending images are not exactly opposite, e.g. they are 39.02° and 40.53° respectively in the case of Figure 10, leading to that the range and location of layover and shadow areas in the ascending and descending images are not precisely complement to each other. Therefore, we need to carefully choose the ascending and descending images for fusion.

2) The DEM used in this experiment has limited accuracy, which causes the errors in shadow and layover extraction.

But we have to bear in mind that for spaceborne systems the incidence angle of SAR image can not be adjusted as we

want, therefore the first reason may always exist. A solution to this problem is to use more images rather than two with one in ascending track and another in descending track for data fusion. For example, we can use 4 images with each 2 in ascending/descending directions. This can be achieved with spaceborne or airborne SAR systems with the ability of adjustable viewing angles. In this case, it will be not a problem to get a totally layover/shadow free orthophoto using the proposed data fusion scheme.

In response to the complex terrain and intrinsic features of SAR slant imaging in mountainous areas, this paper presents a set of methodology to generate color SAR orthophoto, where the images are acquired in both ascending and descending directions and fused together to exclude pixels within layover and shadow regions. The proposed methodology has been tested and validated and has been put into use in the Western China Mapping Project. However, the methodology can be improved further by using more images to get a totally layover/shaodow free fusion, and balancing the tone differences of the images during different side-looking image fusion.

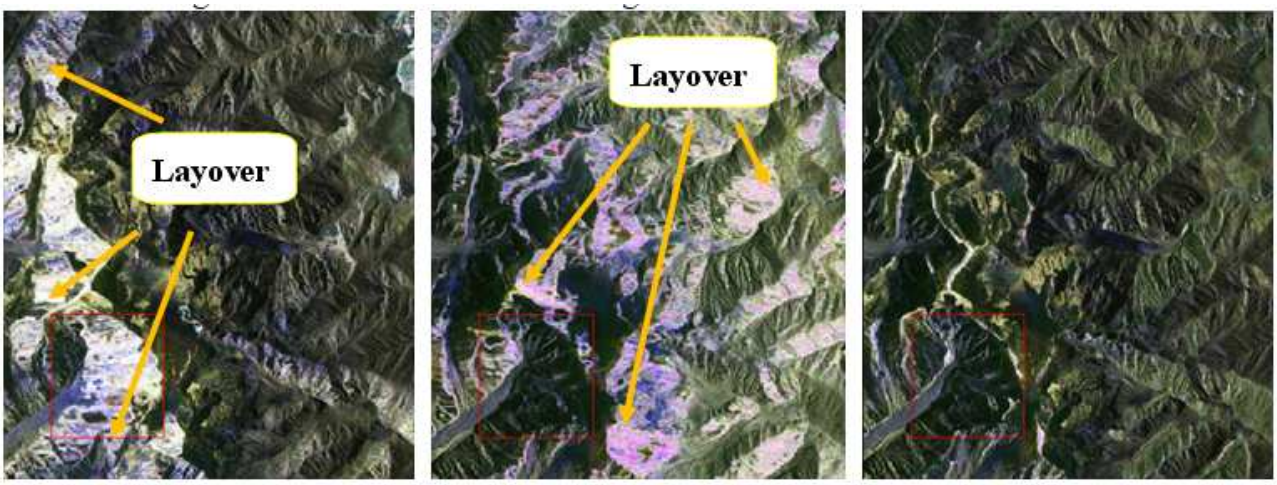

(a) (b) (c)

Figure 10. (a) Rectified ascending RADARSAT-2 image (b) Rectified descending RADARSAT-2 image (c) Ascending and descending RADARSAT-2 image fusion result

REFERENCES

Luckman, A. J., 1998. Correction of SAR Imagery for Variation in Pixel Scattering Area Caused by Topography. *IEEE Transactions on Geoscience and Remote Sensing*, pp. 344-350.

Erxue Chen, Study on Ortho-rectification Methodology of Space-borne Synthetic Aperture Radar Imagery.Thesis (PHD),2004.47-70. Chinese Academy of Forestry.

Erxue Chen, 2002. Space-borne SAR Image Radiometric Correction Algorithm. *High Technology Letters*, pp. 10-14.

Jong-Sen Lee, Mitchell R. Grunes, Thomas L. Ainsworth , Li-Jen Du and Shane R. Cloude., 1999. Unsupervised Classification Using Polarimetric Decomposition and the Complex Wishart Classifier. *IEEE Transactions on Geoscience and Remote Sensing*, 37(5),pp. 2249-2258.

Y. Zhang, J. Zhang and C. Yang, 2002. Terrain induced SAR radiometric distortions and their corrections. *Science of Surveying and Mapping*, 27(4), pp. 23-26.

Y. Zhang and J. Zhang, 2003. A Quasi-automatic rectification method of SAR image based on Image simulation. *Journal of Remote Sensing*, 7(2), pp. 106-111.

Yonghong Jia, 2005. *Data Fusion Techniques for Multisources Remotely Sensed Imagery*. SinoMaps Press, Beijing, pp. 44-48.